Inorganic Chemistry

Forum Article

pubs.acs.org/IC

Lanthanide-Functionalized Nanoparticles as MRI and Luminescent Probes for Sensing and/or Imaging Applications

Steve Comby,*[,†] Esther M. Surender,[†] Oxana Kotova,[†] Laura K. Truman,[†] Jennifer K. Molloy,[†,‡] and Thorfinnur Gunnlaugsson*[,†]

[†]School of Chemistry and Trinity Biomedical Sciences Institute, Trinity College Dublin, Dublin 2, Ireland

[‡]Dipartimento di Chimica "G. Ciamician", Università di Bologna, Via Selmi 2, 40126 Bologna, Italy

Supporting Information

ABSTRACT: The combination of lanthanides and nanoparticles to develop new hybrid nanomaterials has become a highly topical area of research in the field of sensing, biomedical imaging, drug delivery, etc. However, these novel nanomaterials have to be carefully designed to ensure that the unique properties conveyed by each component, i.e., lanthanide ions and nanoparticles, are maximized and not negatively affected by one another. In this Forum Article, the main advances in the design of lanthanide-based nanoparticles will be discussed, with the first part focusing on the design of gadolinium(III)-based nanoparticles and their use as magnetic resonance imaging agents. The second part will then describe the main and most recent designs of luminescent lanthanide-based nanoparticles and their applications as sensors or imaging agents, with a special emphasis on our contribution to this area.

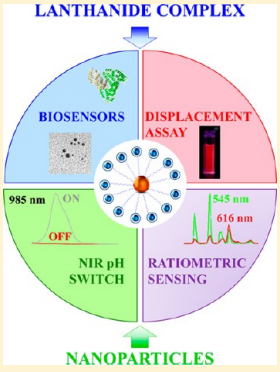

BACKGROUND

The design, development, and synthesis of novel functional hybrid nanomaterials have gained great momentum over recent years in supramolecular chemistry and nanochemistry. Recognized for their potential applications in biotechnology and molecular recognition, in particular sensing and imaging, these nanomaterial systems, which include the likes of quantum dots, nanoscale metal−organic frameworks, and metal nanoparticles (NP), have been successfully employed for drug delivery, in cancer research, and in numerous other applications.[1−8] Owing to their stability, biocompatibility, and intrinsic size- and shape-dependent optoelectronic properties, gold nanoparticles (AuNPs) have been intensively investigated over the past decade as potential sensors for biological substrates as well as imaging and/or therapeutic agents for biomedical applications.[9−17] Moreover, AuNPs have been shown to be easily surface-functionalized with a vast array of organic ligands and biological molecules,[18−20] typically through the use of functional groups such as thiols, amines, or phosphines. This approach yields nanomaterials that are characterized by high surface area to volume ratios. AuNPs have been demonstrated to be both biocompatible and nontoxic, with any unusual toxicity being in most cases associated with the appended ligands (i.e., its chemical nature) rather than the AuNPs themselves. In addition to these appealing properties, the ability to produce hybrid nanomaterials that concentrate such a large amount of magnetically and/or luminescent active probes at their surface has proven to be a very interesting possibility. In other words, high concentrations of active probes are made available, while maintaining a much lower loading of NPs within the biological system. The large number of complexes on the surface of each NP can also promote multiple binding site interactions and thus facilitate the selective targeting of larger biological structures such as DNA, proteins, etc.[1,16] Concomitantly, by exploiting the highly distinctive features of lanthanide ions, their complexes have been used as successful luminescent tools for optical imaging and sensing of biological species.[21−24] The unique magnetic and photophysical properties that the lanthanides possess, such as long-lived excited-state lifetimes and narrow, easily recognizable line-like emission bands at long wavelengths in either the visible or near-infrared (NIR) regions, make them highly attractive in the design of responsive luminescent probes.[25−30] These characteristics are indeed highly desirable for biological applications because autofluorescence and light scattering from biological samples can be overcome using time-resolved detection and, hence, can provide a significant signal-to-noise ratio enhancement compared to that of common organic fluorophores. The surface functionalization of lanthanide(III) complexes onto AuNPs to form biocompatible nanostructures that exhibit unique luminescent properties has not been explored much to date and will be discussed later. Indeed, the majority of the literature encompasses the use of gadolinium(III)-functionalized AuNPs for magnetic resonance imaging (MRI), using ligands such as those shown in Figure 1.

Special Issue: Imaging and Sensing

Received: September 17, 2013
Published: December 19, 2013

   dx.doi.org/10.1021/ic4023568 | Inorg. Chem. 2014, 53, 1867−1879

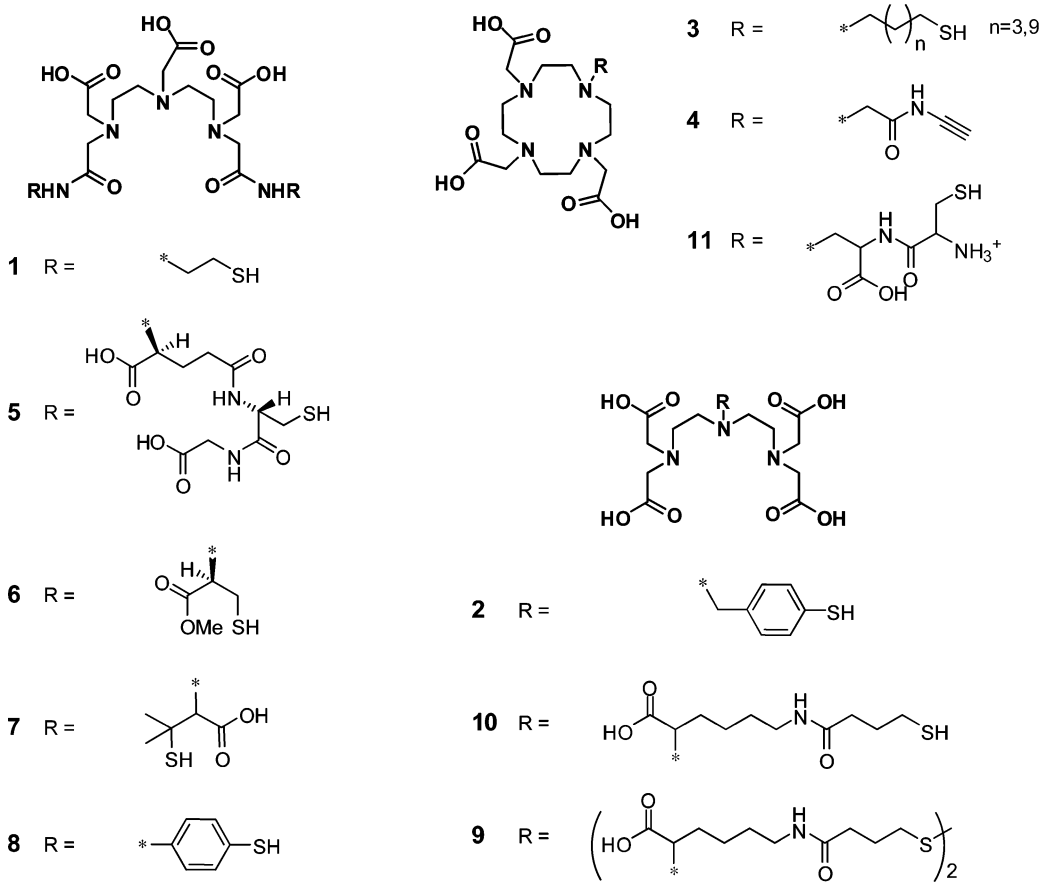

Figure 1. Ligands developed for the design of MRI-active AuNPs.

MRI-ACTIVE LANTHANIDE-FUNCTIONALIZED NPS

To the best of our knowledge, the first example of gadolinium(III)-functionalized AuNPs that were used as potential MRI contrast agents was not reported until early 2006, when Tillement and co-workers showed that a 200-fold gain in relaxivity could be attained from their **1**·Gd-functionalized AuNPs compared to **1**·Gd alone.[31] This system was further applied as a contrast agent for in vivo MRI and X-ray-computed tomography, where the authors demonstrated the ability of such functionalized AuNPs to freely circulate within the blood pool, without detrimental accumulation in the lungs, liver, and spleen.[32] Moriggi et al. reported the use of a simpler thiol derivative, **2**, where the resulting gadolinium(III)-based AuNPs displayed a 5-fold increase in the relaxivity per NP compared to Tillement's initial example.[33] No in vivo studies have been reported for this system to date. To confer water solubility and biological activity to the AuNPs, glyconanoparticles were combined with **3**·Gd complexes for in vitro application. Through variation of the sugar and its position relative to the paramagnetic ion, Marradi and co-workers demonstrated that, using galactose, a 6-fold increase in the relaxivity per millimolar of gadolinium(III) could be achieved compared to that of the commercially available Dotarem.[34,35] Another approach taken by the team of Mirkin and Meade was to utilize CuAAC click chemistry to bind poly dT oligonucleotides to a gadolinium(III) complex, **4**·Gd, which, in turn, could be immobilized onto citrate-stabilized AuNPs. Conjugation to DNA facilitated cell permeability, with a 50-fold increase in the cellular uptake being evident compared to that of Dotarem, while simultaneously providing concomitant enhancement of the relaxivity per NP.[36]

Slight modification of previously reported MRI ligands is becoming more prominent in the literature, with numerous conjugates being reported exhibiting large relaxivity values, such as the gadolinium−DTPA conjugates of glutathione (**5**·Gd),[37] cysteine (**6**·Gd),[38] penicillamine (**7**·Gd),[39] or 4-aminothiophenol (**8**·Gd).[40] To further enhance the relaxivity of such gadolinium(III)-functionalized AuNPs, Chechik and co-workers demonstrated that the MRI-active **9**·Gd and **10**·Gd AuNPs could be further modified by coating the particles with polyelectrolytes, such as poly(ethylene imine), which can self-assemble at the gold surface.[41] However, the polyelectrolyte coating only resulted in enhanced relaxivity for a certain layer thickness, between two and four layers, after which the restricted diffusion of water molecules was shown to be detrimental to the overall relaxivity.[42] Apart from acyclic compounds, 1,4,7,10-tetraazacyclododecane (cyclen) derivatives, such as **4**·Gd and **11**·Gd, have also recently demonstrated great potential in providing high stability and large relaxivities for biological MRI.[36,43] Unlike many acyclic compounds, these cyclen-based systems yield both kinetically inert and thermodynamically stable complexes, which is extremely important for clinical applications of such contrast agents. Having briefly mentioned the diversity of gadolinium(III)-based AuNPs reported so far in the literature for MRI-based imaging, we will now turn our attention to the recent advances made in the design and development of luminescent functionalized NPs, focusing on our main contributions to the field,

dx.doi.org/10.1021/ic4023568 | Inorg. Chem. 2014, 53, 1867−1879

Scheme 1. Luminescent Lanthanide(III)-Functionalized AuNPs Developed for Sensing Applications in the Gunnlaugsson Group

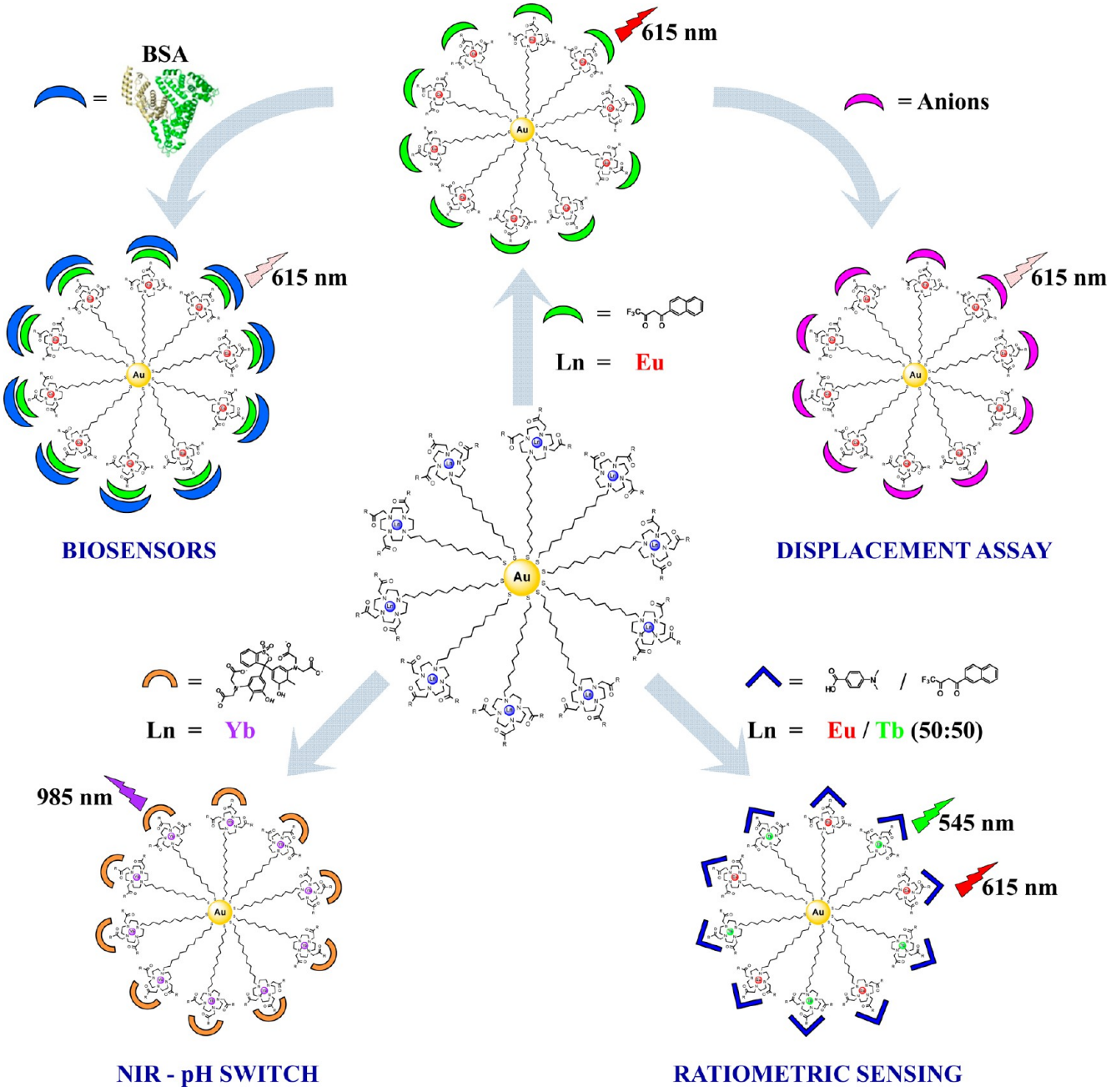

particularly their use as nanoprobes for sensing and/or imaging applications, as summarized in Scheme 1.

LUMINESCENT LANTHANIDE-FUNCTIONALIZED NPS

In recent years, the functionalization of NPs with lanthanide(III) complexes has gained momentum because they are considered as highly attractive nanostructures for the development of novel responsive biological probes for sensing, diagnostics, and medical imaging. Before discussing the surface functionalization of AuNPs with luminescent lanthanide(III) complexes, our main topic of interest in the Gunnlaugsson group, a brief overview of the various types of lanthanide(III)-based NPs employed for sensing and imaging purposes will be given.

Lanthanide-Containing Inorganic, Polymeric, and Silica NPs. Overall, luminescent lanthanide(III) ions have been predominantly incorporated as dopants in inorganic NPs, being usually made from rare-earth oxides, phosphates, or fluorides, and used as linear and/or nonlinear optical probes for biological applications.[44−50] Polymeric lanthanide(III)-based NPs, consisting of lanthanide(III) complexes embedded in polystyrene NPs, have been developed by Härmä and collaborators and successfully applied for nucleic acid diagnostics as well as for heterogeneous and homogeneous bioaffinity assays.[51−54] More recently, the same authors developed a range of NP assays for the determination of protein and cell concentrations.[55−58] Each of these assays was based on time-resolved luminescence resonance energy transfer (TR-LRET), a mechanism that took place from the europium-

dx.doi.org/10.1021/ic4023568 | Inorg. Chem. 2014, 53, 1867−1879

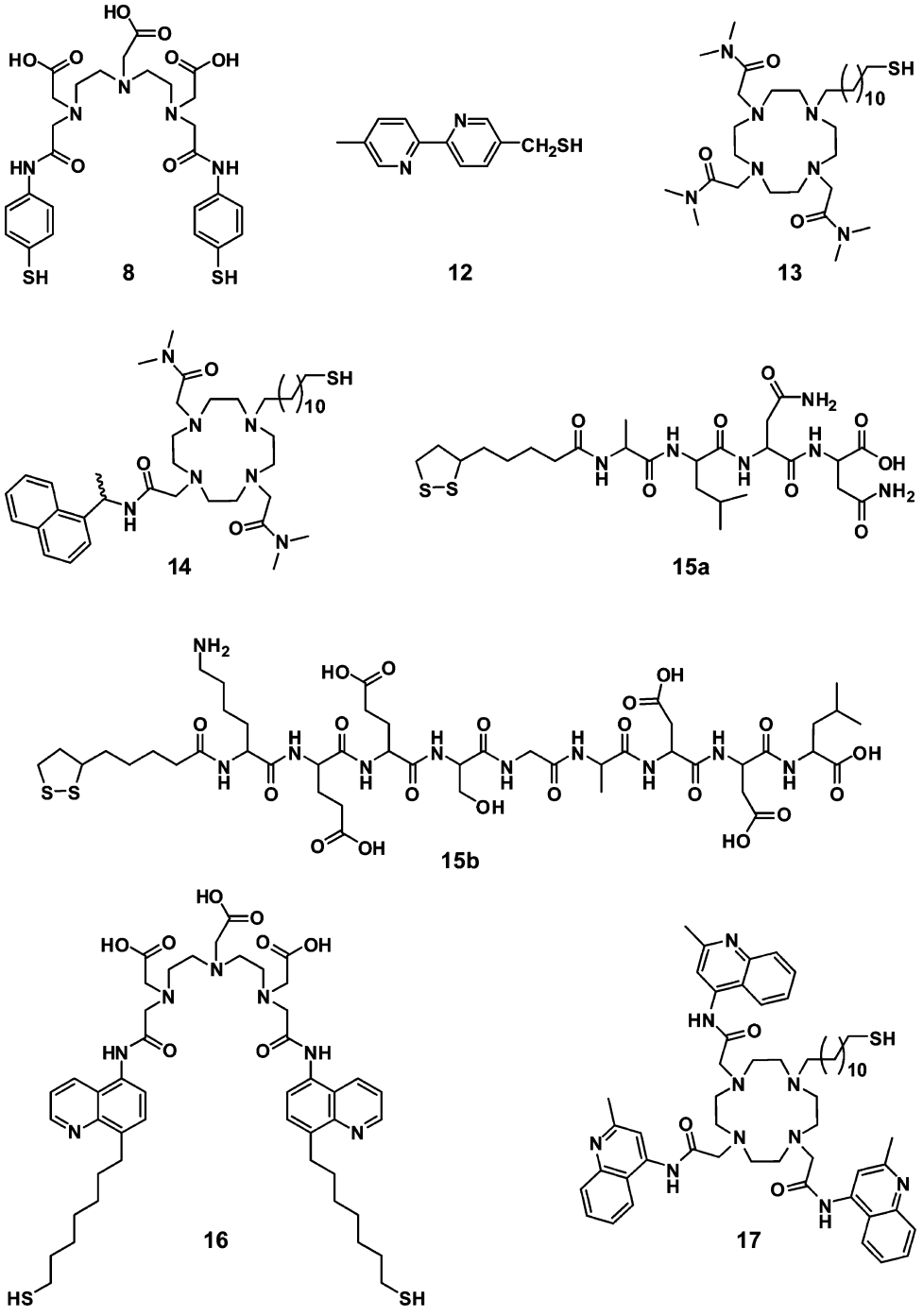

Figure 2. Ligands developed for the design of luminescent AuNPs.

(III)-based polystyrene NPs to diverse acceptors, such as labeled proteins or protein-coated quantum dots.

Despite improved sensitivity compared to that of a single lanthanide(III) chelate, these lanthanide(III)-based polystyrene NPs have a tendency to agglomerate in aqueous solution, and potential chelate leakage has been reported from such systems. In comparison to polystyrene NPs, silica NPs have demonstrated superior water solubility and were consequently used to encapsulate visible- and/or NIR-emitting lanthanide(III) complexes. In most cases, the embedded chelates exhibited enhanced photophysical properties.[59−63] As an alternative to avoid any risk of leakage of the luminescent labels, the lanthanide(III) complexes were covalently linked to the NP surface, taking advantage of the possibility of chemically modifying the silanol surface through successive organic reactions.[64−68] Such silica-based NPs that have been either doped or surface-functionalized with lanthanide(III) chelates were successfully used in immunoassays or directly applied in time-resolved fluorimetric assays, demonstrating that streptavidin−biotin technology can be adapted to these new types of labels.[69−71] Further applications as luminescent sensors for glucose,[72] DNA,[73] prostate-specific, or hepatitis B surface antigens[74,75] were reported, while concomitantly demonstrating their suitability as time-gated luminescence imaging probes in living cells and tissues[76,77] or for two-photon luminescence imaging.[78] These highlights clearly validate the scope of using

dx.doi.org/10.1021/ic4023568 | Inorg. Chem. 2014, 53, 1867−1879

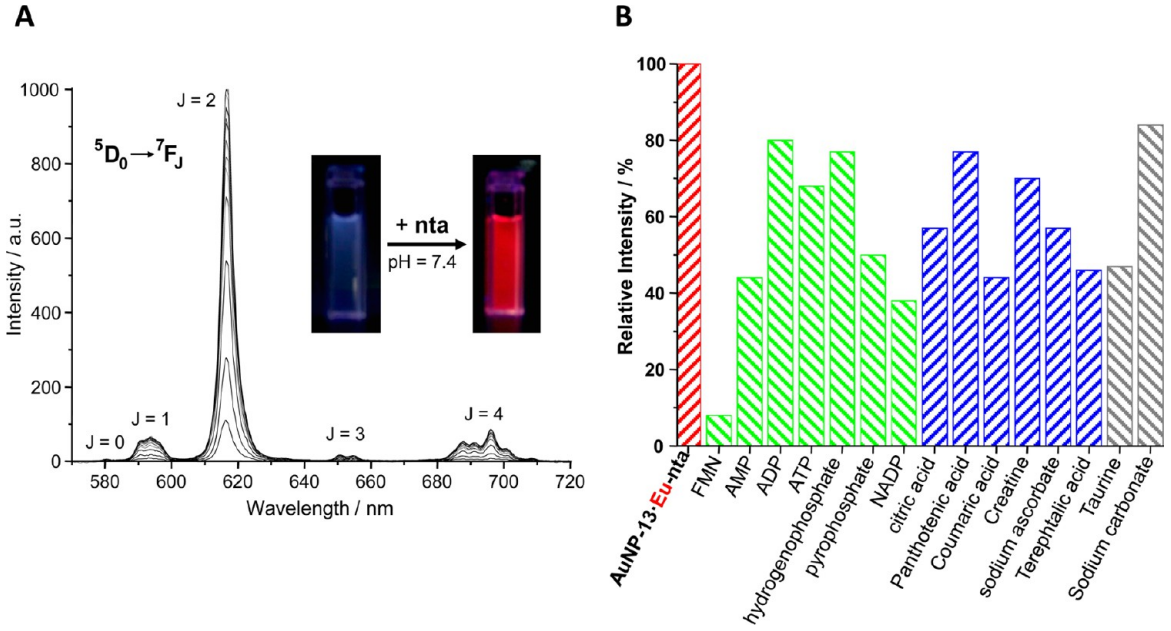

Figure 3. (A) Changes in the europium(III)-centered emission of AuNP−**13**·Eu in a HEPES buffer (pH 7.4) upon the addition of nta (0−500 equiv) at 298 K (λ_{ex} = 330 nm). Inset: Emission arising from a solution of AuNP−**13**·Eu under a UV−vis lamp (λ_{ex} = 365 nm) before and after the addition of nta. (B) Bar chart diagram representing the europium(III)-centered emission quenching, in percent, observed upon the addition of biologically relevant anions to a AuNP−**13**·Eu−nta solution. [AuNP−**13**·Eu] = 10^{-7} M; [nta] = 1.2×10^{-5} M.

lanthanide-emitting NPs for biological use. The great potential of such systems was further emphasized by a recent study by Ai et al., where lanthanide(III)-based silica NPs allowing for the rapid and ultrasensitive detection of an anthrax biomarker were engineered to deal with the threat of biological attacks.[79]

Lanthanide-Functionalized AuNPs. While the beneficial attributes of noble-metal NPs have been previously mentioned, only a few examples of lanthanide(III)-functionalized silver nanoparticles (AgNPs) or AuNPs have been developed to date. To the best of our knowledge, the first example of lanthanide(III)-functionalized AgNPs was reported by Sun et al. in 2005 and was obtained by coating the NPs with a well-known tris[europium(III) β-diketonate], Eu(tta)$_3$. However, emission of the resulting NPs was as intense as that of the simple lanthanide(III) chelate, with significant surface-enhanced luminescence being canceled by the quenching effect of the AgNPs.[80] To take full advantage of the metal-enhanced fluorescence, core−shell silver−silica NPs were developed and displayed improved luminescence characteristics for both organic dyes and europium(III) chelates.[81] Protein-coated AgNPs have also been made, in which the lanthanide(III) chelate that is formed with a biocytinamide ligand binds to the coated NPs only in the presence of streptavidin. Modulation of lanthanide(III) chelate emission in the presence of AgNPs served as a proof of principle for exploiting surface enhancement in proximity assays.[82] Concomitantly, AuNPs have attracted considerable interest for biological applications, not only because of their desirable biocompatibility but also because they have been shown to be readily internalized by human cells.[83−88] While it has been well-documented that the preferred pathway for internalization of AuNPs is through endocytosis, recent studies have investigated different approaches to circumvent this uptake route and successfully shown that at least a fraction of the particles internalized are within the cytosol. Through cytosol pathways such as direct membrane translocation, specific sites within the cells can be directly targeted, validating the application of AuNPs as intracellular probes and agents.[85,88] The functionalization of AuNPs with lanthanide(III) chelates to potentially act as bioprobes is, however, still a very novel area of research, which can be separated into two main categories: gadolinium(III)-based NPs for MRI applications[31−43] and luminescent lanthanide(III)-based NPs for sensing and imaging purposes. Having briefly mentioned the major gadolinium(III)-based AuNP systems reported in the literature to date in the above section, we focus our attention here toward luminescent lanthanide(III)-based AuNPs (Figure 2). The first two examples of AuNPs conjugated to luminescent lanthanide(III) complexes were published in 2006. In both studies, the lanthanide(III) chelates were conjugated to the AuNP surface via a short thiol linker, yielding luminescent lanthanide(III)-based AuNPs. Ipe et al. used the CH_2-spaced 2,2′-dipyridyl ligand **12** with europium(III) and terbium(III) to form 1:3 (lanthanide−ligand) complexes on the AuNP surface in acetonitrile,[89] while Lewis et al. used the europium(III) diethylenetriaminepentaacetic acid based complex **8**·Eu, which was linked to the AuNPs via thiophenol spacers.[90] The former system has been investigated as a potential sensor for metal ions because the addition of calcium(II), magnesium(II) to a certain extent, and, more importantly, nickel(II), copper(II), and zinc(II) resulted in the quenching of lanthanide(III)-centered emission, being most likely due to displacement of the lanthanide(III) ions from the binding cavity.

Conversely, the combination of AuNPs and lanthanides for sensing applications in aqueous solution was first reported by Gunnlaugsson and co-workers, where the C_{12} alkylthiol-modified europium(III) cyclen complex, **13**·Eu, was grafted onto ∼5 nm AuNPs and applied for the time-resolved luminescence sensing of anions such as biologically relevant phosphates in aqueous solution [*N*-(2-hydroxyethyl)piperazine-*N*′-2-ethanesulfonic acid (HEPES), pH 7.4].[91] This work differentiated itself from the previous examples because it relied

dx.doi.org/10.1021/ic4023568 | *Inorg. Chem.* 2014, 53, 1867−1879

on the use of kinetically inert and thermodynamically stable macrocyclic lanthanide(III) cyclen complexes and, more importantly, on the use of a much longer thiol linker. The choice of the C_{12} alkylthiol linker was made with the intention of minimizing the quenching of luminescence from the gold surface[92−94] as the efficiency of AuNP-induced luminescence quenching has been demonstrated to be strongly distance-dependent.[95−98] The key to this development was the successful synthesis of the thiol-substituted cyclen complex **13**·Eu, which enabled its covalent attachment onto the surface of AuNPs in an efficient manner, resulting in the formation of water-soluble AuNP−**13**·Eu, which were found to be stable in a buffered aqueous solution over a period of many months. The absence of a chromophore or antenna in this system, combined with the presence of two metal-bound water molecules that can efficiently quench the europium(III) excited state, gave rise to NPs that were almost nonluminescent. However, the addition of a well-suited antenna (namely, one that has a high affinity for the lanthanide(III) ions, being able to displace the aforementioned metal-bound water molecules as well as having desirable singlet and triplet excited-state energies for sensitizing the lanthanide excited states), such as 4,4,4-trifluoro-1-(2-naphthyl)butane-1,3-dione (nta), to the water-soluble europium(III)-functionalized AuNPs resulted in the formation of highly red-emitting ternary complexes on the AuNP surface upon direct excitation of the antenna. The characteristic europium(III)-centered emission displayed a particularly intense $\Delta J = 2$ transition (Figure 3A), reflecting direct coordination of the nta antenna to the europium(III) ions. Moreover, the pK_a of the first deprotonation of the α-proton of nta to yield the β-diketonate was determined to be ca. 7, corroborating the formation of strong ternary complexes between **13**·Eu and nta around that pH. This also justified the fact that europium(III) emission was found to be highly pH-dependent.[99] As the formation of such luminescent ternary assemblies onto the AuNP surface is dynamic, the resulting luminescent AuNPs were successfully applied in displacement assays for the sensing of biologically relevant anions, such as flavin mononucleotide (FMN), whereby the antenna could be replaced/displaced by FMN, which led to a quenching ("switch off") of europium(III) emission. Overall, the luminescence quenching was found to be optimal for FMN, while being generally stronger for phosphate-containing biomolecules compared to other functionalities such as carbonates or carboxylates (Figure 3B).[91]

This particular system was shown to behave in a similar manner when attached to a flat gold surface; emission of the europium(III) center was greatly enhanced upon the addition of nta, demonstrating that the use of ternary complexes in such systems is highly attractive for sensing applications.[100] More recently, the introduction of a chiral moiety on the initial lanthanide(III) complex design afforded water-soluble luminescent chiral NPs, AuNP−**14**·Eu, which were shown to interact with chiral molecules such as amino acids. Retention of the chirality upon functionalization onto the gold surface was confirmed by circular dichroism, with the spectra of the enantiomeric pair displaying a mirror image behavior. Unfortunately, circularly polarized emission was too weak to be measured accurately in this case, possibly because of quenching induced by the gold surface. Preliminary results demonstrated the successful luminescent detection of chiral amino acids such as histidine and tryptophan, emphasizing the potential of AuNP−**14**·Eu to act as a chiral nanoprobe.[101]

After directing our main interest purely toward sensing applications of small single molecules or ions, it was important to move further and study the interaction of such functionalized NPs with larger substrates such as biomolecules (e.g., enzymes, proteins, etc.) in an effective and reliable way, extending this work toward in vivo imaging applications. Indeed, with the nanoprobes developed having comparable sizes to biomolecules, it is crucial to understand how they interact with proteins and what the resulting positive and/or negative outcomes of such interactions are.[102−106] Of particular interest are serum proteins, such as albumin, which always play an important role by interacting with the imaging agent. Consequently, we have been evaluating the interaction of the luminescent europium(III)-functionalized AuNPs, AuNP−**13**·Eu−nta, with bovine serum albumin (BSA). Europium(III) emission arising from the luminescent AuNPs was almost completely quenched upon the addition of BSA. In-depth analysis of this quenching event demonstrated that this was neither due to replacement of the complex from the gold surface nor due to displacement of the antenna from the ternary system as shown earlier but rather was the result of the strong noncovalent interaction taking place between the nta antenna and BSA.[107] Apart from determining that BSA had a high binding affinity for the antenna and could indeed accurately report the binding of small molecules with proteins through quenching of the europium(III)-centered emission, synchronous fluorescence and circular dichroism spectroscopies were used to demonstrate that the protein secondary structure was not affected upon binding with the surface-functionalized AuNPs. On the basis of the results obtained, the overall system in the presence of BSA, AuNP−**13**·Eu−nta−BSA, was used as a biosensor for luminescent detection of conventional drugs via perturbation of the NP−protein interaction. The addition of the competitive drug ibuprofen switched "on" the previously quenched europium(III) emission, permitting localization of the compound in site II of BSA. More importantly, the presence of warfarin, a site I drug, did not interfere with the detection of ibuprofen, which further emphasized the potential of this system being applied to biomedical fields.

To gain further insight into the interaction of NPs with living systems, Pikramenou and co-workers have been investigating the potential DNA damage that can be induced by such NPs, in this particular case using cerium(III)- and europium(III)-based AuNPs. The authors showed that high-resolution synchrotron X-ray fluorescence microscopy was a very sensitive technique to investigate the intracellular localization of the lanthanide(III)-based NPs in human fibroblasts as well as to screen the genotoxicity of the NPs once internalized.[108] Following their interest in the delivery of NPs in cells using lanthanide(III) luminescent active probes, the same group reported the synthesis of water-soluble peptide-coated AuNPs and investigated the binding of lanthanide(III) ions to peptides **15a** and **15b** at the surface of the coated NPs.[109] More recently, Pikramenou and collaborators brought the approach a step further by coating AuNPs with europium(III) complexes bearing quinoline chromophoric units, **16**·Eu, for efficient sensitization of europium(III) emission and a pH low insertion peptide (pHLIP). The co-coated NPs were demonstrated to address labeling issues in platelets for live cell imaging by using a peptide-induced pH-dependent delivery mechanism that enabled rapid uptake of the modified NPs in cells. The translocation of pHLIP across the membrane in low-pH conditions (pH $\leq$6.5) was shown to be responsible for the fact

dx.doi.org/10.1021/ic4023568 | Inorg. Chem. 2014, 53, 1867−1879

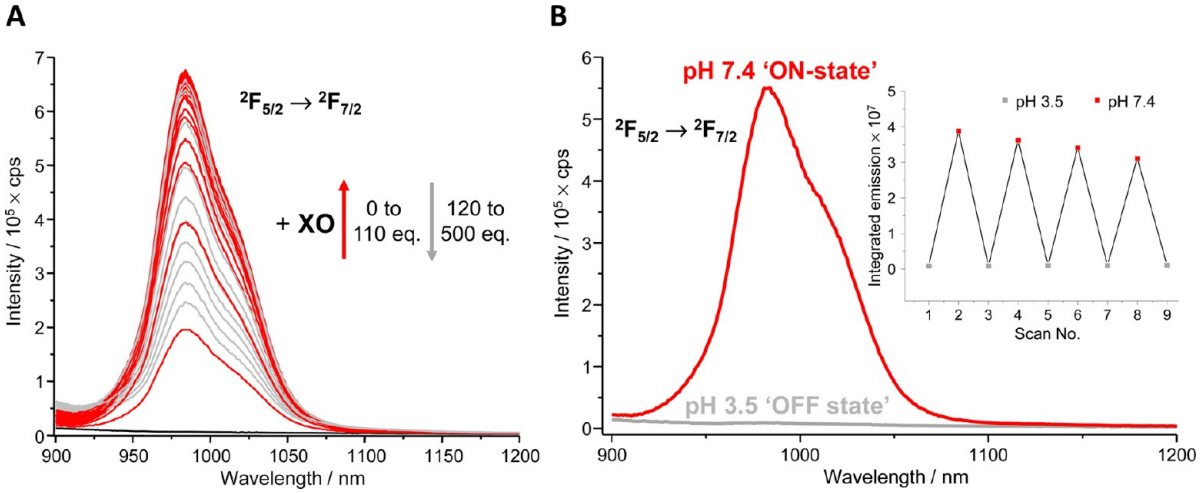

Figure 4. (A) Changes in the ytterbium(III)-centered NIR emission of AuNP−**13**·Yb in a HEPES buffer (pH 7.4) upon the addition of XO (0−500 equiv) at 298 K (λ_{ex} = 580 nm). (B) Changes in the ytterbium(III)-centered NIR emission of AuNP−**13**·Yb−XO between pH 7.4 and 3.5. Inset: "on-off" NIR switch behavior between pH 7.4 and 3.5. [AuNP−**13**·Yb] = 10^{-7} M; [XO] = 3×10^{-6} M.

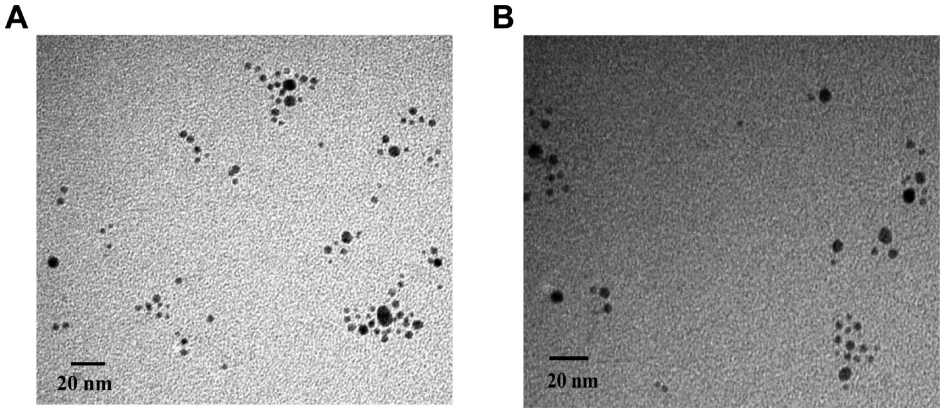

Figure 5. TEM images for (A) AuNP−**17**·Eu and (B) AuNP−**17**·Eu/**17**·Tb.

that the functionalized NPs only entered platelets at this pH and not at pH 7.4.[110] These results clearly demonstrate the potential of lanthanide(III)-functionalized AuNPs as luminescent probes in biological and medical applications.

All of the examples discussed so far have been focusing on the use of visible-emitting europium(III) or terbium(III) complexes. However, luminescent probes displaying emission in the NIR are particularly valuable for medical imaging because of the increased tissue transparency and reduced interferences from light scattering and biological autofluorescence at these wavelengths. Moreover, the low-lying excited states of the NIR-emitting lanthanide(III) ions allow for their sensitization using visibly absorbing antennae, which is a major advantage over their visible-emitting counterparts discussed above. Despite these advantages, it is only recently that the first example of NIR-emitting lanthanide(III)-functionalized AuNPs was published by Gunnlaugsson and co-workers.[111] In this particular work, the approach for the synthesis of AuNPs was modified, and the tetraoctylammonium bromide stabilized NPs in toluene were transferred into an aqueous phase by direct ligand exchange using the thiol-alkylated lanthanide(III) cyclen complex, without the need for the intermediate phase-transfer step involving 4-(dimethylamino)pyridine. The addition of xylenol orange (XO) to the ytterbium(III)-functionalized NPs, AuNP−**13**·Yb, resulted in the formation of ternary complexes at the gold surface, which upon excitation of XO at 580 nm gave rise to the characteristic ytterbium(III)-centered emission in the 900−1200 nm range, as shown in Figure 4A. NIR emission of the resulting AuNP−**13**·Yb−XO displayed pH-induced modulation, with 14-fold enhancement of the luminescence signal being observed when going from acidic conditions (pH ≤4) to physiological pH. In addition, the emission arising from AuNP−**13**·Yb−XO was shown to be reversibly switched "on" and "off" as a function of the pH over several cycles, enabling these luminescent AuNPs to function as a supramolecular NIR switch (Figure 4B).[111]

These aforementioned results demonstrated that AuNPs can be, in principle, easily modified by bringing new functionalities via surface functionalization and thus tailoring their overall properties as a function of the biological process under investigation.

Lanthanide-Functionalized NPs for Multimodal Imaging. The versatility of these nanoprobes is particularly valuable for the development of multimodal imaging probes. This was achieved recently in our group by co-coating the AuNP surface with a 50:50 mixture of europium(III) and terbium(III) complexes formed with the cyclen-based ligand **17**. It was demonstrated by transmission electron microscopy (TEM) and dynamic light scattering that the multiple coating did not affect the particle size and distribution because they were comparable

dx.doi.org/10.1021/ic4023568 | Inorg. Chem. 2014, 53, 1867−1879

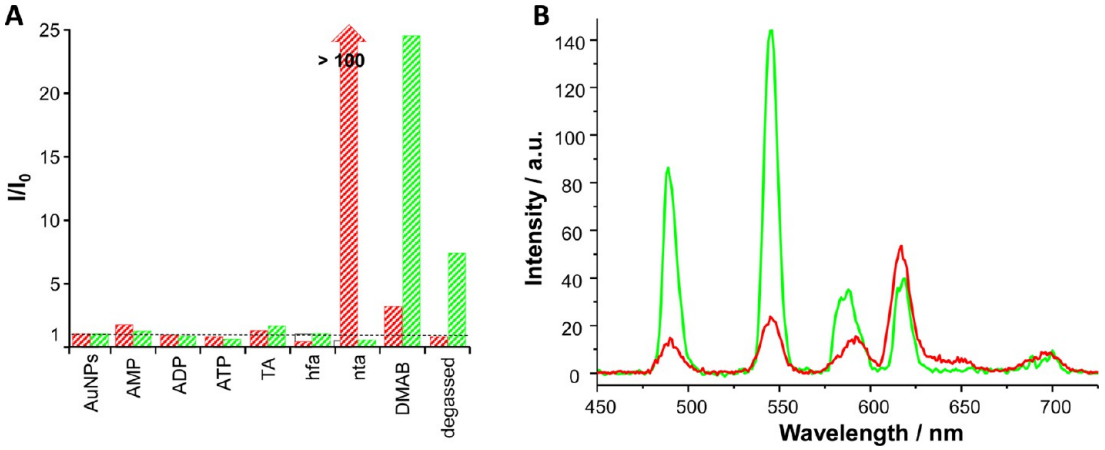

Figure 6. (A) Changes in europium(III) and terbium(III) emission of AuNP−**17**·Eu/**17**·Tb at 615 and 545 nm, respectively, upon the addition of various analytes; TA = terephthalic acid, hfa = 1,1,1,5,5,5-hexafluoro-2,4-pentanedione, and DMAB = (dimethylamino)benzoic acid. (B) Emission spectra of AuNP−**17**·Eu/**17**·Tb under aerated (red line) and degassed (green line) conditions.

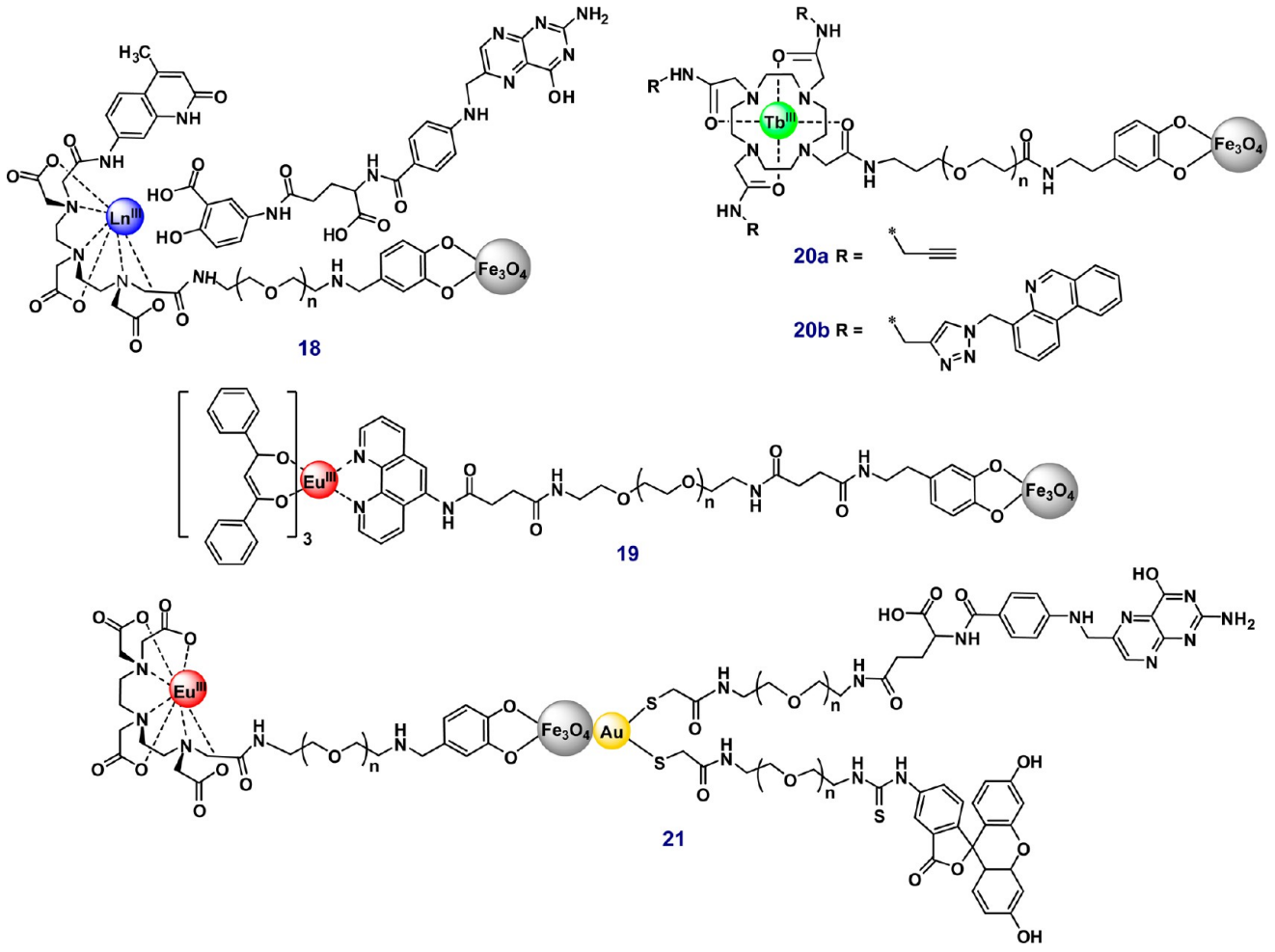

Figure 7. Lanthanide(III)-based complexes developed for the functionalization of Fe_3O_4 and Au−Fe_3O_4 NPs.

to that observed for the single-coated NPs, e.g., AuNP−**17**·Eu (Figure 5). Upon excitation of the quinaldine chromophoric units of **17**, the AuNP−**17**·Eu/**17**·Tb system displayed the characteristic green and red emissions of terbium(III) and europium(III), respectively, confirming the dual-emissive nature of the functionalized AuNPs and their potential for ratiometric sensing of biologically relevant analytes. The pH dependency of AuNP−**17**·Eu/**17**·Tb was established and showed that both europium(III)- and terbium(III)-centered emissions were switched "on" in the physiological pH range, while being switched "off" in acidic and basic conditions.

Moreover, by the careful selection of two antennae, 4-(dimethylamino)benzoic acid (DMAB), which sensitizes terbium(III), and nta, which sensitizes europium(III), this

dx.doi.org/10.1021/ic4023568 | Inorg. Chem. 2014, 53, 1867−1879

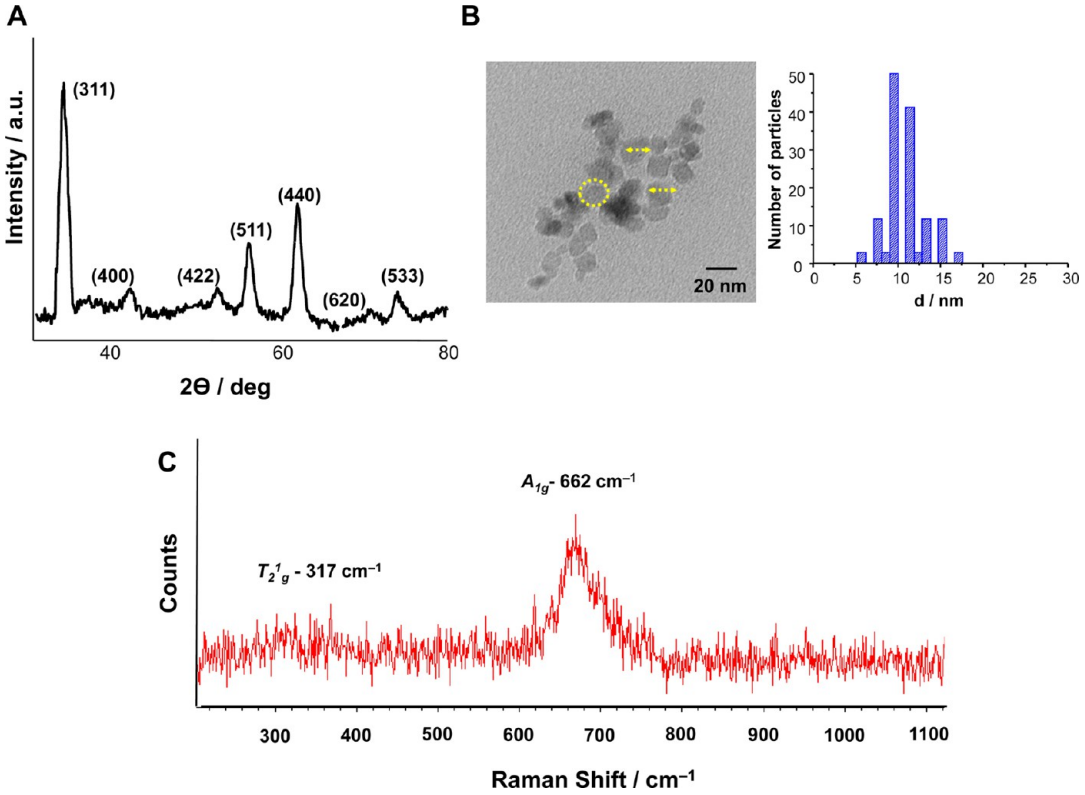

Figure 8. Characterization of the as-synthesized Fe_3O_4 NPs. (A) XRD pattern. (B) TEM image and size-distribution histogram. (C) Raman spectra.

water-soluble system showed potential application as a logic gate, with the ability to either switch "on" europium(III) or terbium(III) emission independently of one another (Figure 6A). Indeed, the outputs can be described in molecular logic-gate terms, where emission at three different wavelengths can be defined in terms of Boolean algebra, corresponding to the NAND, NOR, and NOT functions.[112] Consequently, the presence or absence of oxygen as an input was also shown to affect the logic behavior of the system, with degassed solutions displaying a ratiometric 6-fold increase in the terbium(III)-centered emission alone; the europium(III) $^5D_0 \rightarrow {}^7F_4$ transition at 700 nm remained unchanged and was thus selected as the internal reference (Figure 6B). This ratiometric response using dual europium(III)−terbium(III)-based probes has been well documented in the literature,[113−116] but their incorporation onto one single AuNP nanoprobe is, to the best of our knowledge, a first.[117]

Apart from dual-emissive systems, the development of multifunctional nanoprobes containing magnetically and optically active components has gained momentum because biological imaging and selective recognition can be achieved simultaneously in such systems.[118−121] Very few examples of such systems using magnetite (Fe_3O_4 NPs) or gold−magnetite (Au−Fe_3O_4 NPs) nanoparticles as the magnetically active component and lanthanide(III) complexes as the luminescent-responsive unit have been developed to date (Figure 7).[122−127] The general approach relies on the synthesis of poly(ethylene glycol) (PEG) polymer derivatives, which have been terminated with a dopamine chelator, thus enabling surface functionalization of the Fe_3O_4 NPs. The resulting Fe_3O_4−PEG conjugates were further functionalized with lanthanide(III) complexes using standard coupling reactions. Yang and collaborators followed a slightly different approach and used folic acid conjugated terbium(III) and europium(III) complexes to functionalize Fe_3O_4 NPs (**18**), enabling targeted fluorescence in vitro imaging of HeLa cells that overexpressed the folate receptor.[122,124] The same system functionalized with gadolinium(III) complexes displayed larger relaxivities compared to the standard MRI agent Magnevist.

Xi et al. reported a simple and versatile strategy to transform hydrophobic Fe_3O_4 NPs into hydrophilic and biocompatible dual functional assemblies, which can function as sensitive probes for both MRI and luminescent imaging (**19**).[123] This approach was also utilized by Pierre and co-workers, who demonstrated that Fe_3O_4 NP assemblies functionalized with terbium(III) cyclen complexes can also show promise for dual imaging by MRI and time-gated luminescence spectroscopy (**20a** and **20b**).[125] Moreover, the cyclen complex **20a** containing acetylene functional groups further gave this assembly the unique opportunity to be readily conjugated to azide-functionalized biomolecules, such as proteins and oligonucleotides, directly in a cellular environment by copper-(I)-catalyzed Huisgen cycloaddition. The same research group has taken this approach further and recently reported the formation of magnetoluminescent light switches, where Fe_3O_4 NPs have been functionalized with two different metallointercalators such as a ruthenium complex and a europium-(III) cyclen analogue to **20b**. These ruthenium(II)-/europium-(III)-based Fe_3O_4 NPs were used as efficient dual-responsive probes by both luminescence and relaxivity measurements.[126] The luminescence response was shown to be dependent on the metallointercalator; on the one hand, the ruthenium(II) complexes acted as a "turn-on" light switch upon intercalation in the DNA helix, while, on the other hand, the europium(III) complex behaved as an efficient "turn-off" switch. Such an approach to the incorporation of ruthenium(II) complexes at

dx.doi.org/10.1021/ic4023568 | Inorg. Chem. 2014, 53, 1867−1879

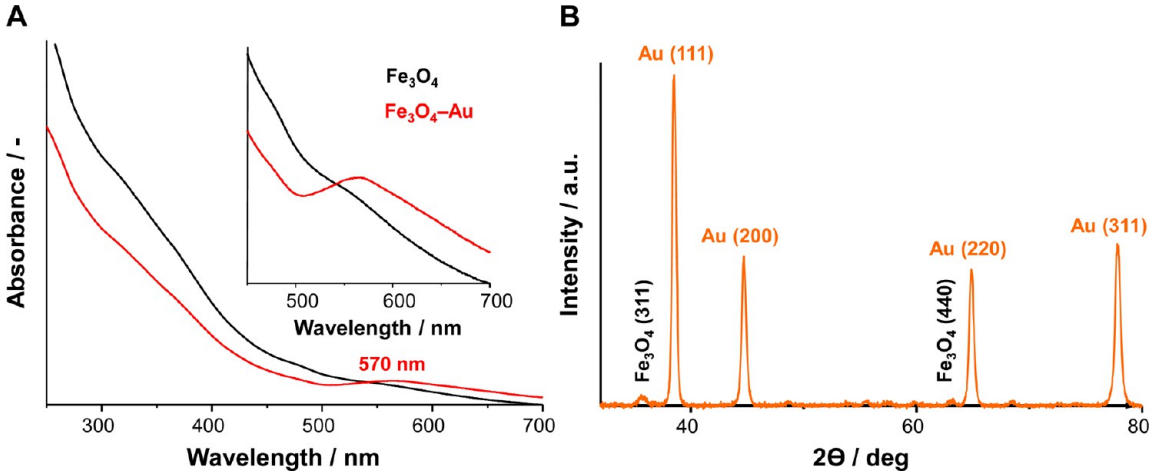

Figure 9. (A) UV−vis absorption spectra of Fe_3O_4 and Au−Fe_3O_4 NPs. (B) XRD pattern of Au−Fe_3O_4 NPs.

the surface of NPs as DNA targeting motifs was, to the best of our knowledge, first reported by Gunnlaugsson and co-workers, where ruthenium(II)-stabilized AuNPs have been used.[128]

Recently, a novel type of multifunctional nanoprobe has been developed by Wang and co-workers using dumbbell-like Au−Fe_3O_4 NPs. The Fe_3O_4 part of the dumbbell-like NPs was functionalized with an europium(III) complex, while fluorescein isothiocyanate and folic acid containing thiol ligands were attached to the gold surface (**21**).[127] The overall system was shown to act as a MRI/fluorescence dual-modal imaging probe as well as allowing for cancer cells to be counted by colorimetric/fluorigenic dual-modal detection, reaching detection limits as low as 100 cells.

A similar approach was followed by our research group, where we proposed to use core−shell Au−Fe_3O_4 NPs instead of dumbbell-like NPs. The core−shell Au−Fe_3O_4 NPs were synthesized according to the iterative hydroxylamine seeding approach reported by Lyon et al., where Fe_3O_4 NPs were obtained using the co-precipitation approach and gold shells were formed using the iterative hydroxylamine seeding procedure.[129] The main advantages of the core−shell Au−Fe_3O_4 NPs compared to the conventional Fe_3O_4 NPs are that they (i) possess enhanced chemical stability because the iron core is protected from oxidation and corrosion, (ii) contain both magnetic and optically active plasmonic units, and, more importantly, (iii) the gold surface facilitates the attachment of different molecules or complexes via thiol chemistry.

At first, the composition of Fe_3O_4 NPs was ascertained using IR spectroscopy, powder X-ray diffraction (XRD) analysis, and Raman spectroscopy. The composition of Fe_3O_4 NPs can vary considerably depending on the preparation protocol as well as on the experimental conditions of their analysis because of the possible formation of ferrimagnetic maghemite (γ-Fe_2O_3) as the byproduct.[130] The X-ray patterns of γ-Fe_2O_3 and Fe_3O_4 are very similar to one another, thus rendering XRD analysis of such NPs difficult.[131]

All of the reflection peaks observed in the XRD pattern (Figure 8A) were assigned to a spinel structure with the characteristic reflections of iron oxide (Fe_3O_4 or γ-Fe_2O_3). No diffraction peaks from hematite, iron oxyhydroxides, hydroxides, or other impurities were found. TEM images of Fe_3O_4 NPs showed the presence of spherical particles with an average diameter of ∼9−12 nm (Figure 8B), with the narrow size distribution confirming that the particles are essentially monodisperse. To identify the exact phase composition of the synthesized NPs, Raman spectroscopy, which has been extensively used to differentiate iron oxides, especially magnetite and maghemite, was used.[132] Raman spectra of Fe_3O_4 NPs, shown in Figure 8C, displayed two bands at 662 cm^{-1} (A_{1g}) and 317 cm^{-1} (T_{2g}^{1}). These bands, characteristic of magnetite only, are consistent with the values reported in the literature, confirming that the black product obtained after synthesis is a pure magnetite phase. These core−shell Au−Fe_3O_4 NPs were characterized by UV−vis absorption spectroscopy, XRD, and scanning electron microscopy (SEM) including energy-dispersive X-ray (EDX) spectroscopy analysis.

The UV−vis absorption spectra of core−shell Au−Fe_3O_4 NPs (Figure 9A) displayed an absorption band at 570 nm that is absent from the spectra of the simple Fe_3O_4 NPs. This absorption band, characteristic of the surface plasmon resonance band observed for AuNPs, confirmed the coating of the Fe_3O_4 NP surface by gold. XRD patterns of Fe_3O_4 and Au−Fe_3O_4 NPs along with evolution of the diffraction peaks from gold are also presented in Figure 9B. Further investigation of the Au−Fe_3O_4 NP composition was achieved using SEM, especially EDX analysis. SEM images of the Au−Fe_3O_4 NPs synthesized showed the presence of NPs with a size of ∼100 nm, which can be caused by agglomeration due to precipitation from the solution; see Figure S6A in the Supporting Information. EDX analysis of Au−Fe_3O_4 NPs (Figure S6B in the Supporting Information) showed the presence of gold, iron, and oxygen, with the atomic ratio between iron and gold near 18:1 indicating that the hybrid NPs contained both Fe_3O_4 and gold. The various analytical techniques used for characterization of Au−Fe_3O_4 NPs demonstrated that the required core−shell structures were obtained. The functionalization of Au−Fe_3O_4 NPs was performed in aqueous solution by mixing Au−Fe_3O_4 NPs with **13**·Eu under sonication. The excess of NPs was then removed by precipitation, so that only the Au−Fe_3O_4 NPs that were functionalized with the **13**·Eu remained in solution. The as-functionalized NPs were then used for luminescence titrations, where increasing amounts of the antenna, nta, were added.

The characteristic europium(III) emission observed upon excitation into the diketonate at 330 nm clearly demonstrated binding of the antenna to **13**·Eu and, therefore, formation of the luminescent ternary complex AuNP-**13**·Eu−nta at the surface of Au−Fe_3O_4 NPs (Figure 10A), in a manner similar to

dx.doi.org/10.1021/ic4023568 | Inorg. Chem. 2014, 53, 1867−1879

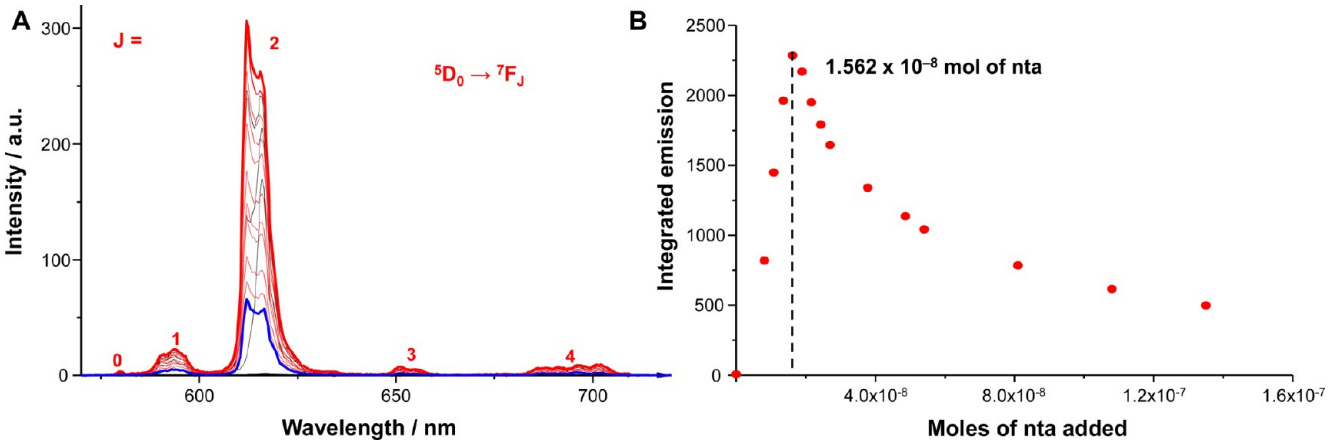

Figure 10. (A) Changes in the europium(III) emission of **13**·Eu–Au–Fe_2O_3 NPs with nta in a HEPES buffer solution (0.1 M, pH 7.4) at 298 K. (B) Changes in the integrated emission for the $^5D_0 \rightarrow {}^7F_2$ transition (604–635 nm) versus moles of nta added.

that seen above for the AuNPs. Furthermore, the intensity changes in the europium(III) transitions were plotted and appeared to reach a maximum at around 0.7 equiv of nta compared to the **13**·Eu concentration, as shown in Figure 10B. The luminescence intensity of **13**·Eu–nta–Au–Fe_3O_4 NPs was calculated to be ~3 times lower than the one observed for **13**·Eu–nta in solution, supporting the quenching effect of the NPs. For this system, the Eu($^5D_0$) excited-state lifetimes were measured in the presence of various concentrations of nta, and the values were in good agreement with those obtained for the previously described AuNP–**13**·Eu complexes.[91] Overall, these results show that Fe_3O_4 or Au–Fe_3O_4 NPs have been shown to be excellent candidates as dual optical–magnetic imaging agents, but at the same time, their synthesis has been particularly challenging, with the characterization of such systems still remaining difficult, and this we are still undertaking in our laboratory.

CONCLUSION

Combining the advantages of lanthanides and NPs in one single hybrid nanomaterial represents an attractive opportunity to develop a whole range of novel luminescent and/or magnetic probes that could find applications as sensors and imaging agents. Such lanthanide-based NPs have demonstrated in most cases enhanced responses to particular biological processes or events compared to the corresponding lanthanide complexes as high concentrations of the active probes are made available at the surface of these NPs. While this field of research is very young, many encouraging and exciting results have emerged among the systems developed to date, which will fuel progress in this area. Gadolinium(III)-based NPs, especially AuNPs, have repeatedly shown much higher relaxivities per millimolar of gadolinium(III) than the ones observed for the gadolinium(III) complexes themselves, while maintaining a much lower loading of NPs within the biological system. Luminescent lanthanide complexes have also been conjugated to various types of NPs, including polystyrene, silica, silver, gold, and magnetite, and the resulting hybrid nanomaterials were then applied in diverse imaging and sensing assays, taking advantage of the time-resolved lanthanide(III)-centered emission. Although considerable advances have been made in the development of lanthanide-based NPs, the understanding of the interaction of such promising nanomaterials with the biological system and their fate in vivo still require strong and consistent attention from the international scientific community. We and others are playing an active role in this field of research, and we look forward to contributing to its development in the future. The above examples, some of which are presented for the first time, demonstrate the breath of variety that these systems have to offer.

ASSOCIATED CONTENT

Supporting Information

Experimental section, spectrophotometric titration protocols and general analytical instrumentation used, synthesis and characterization of ligands **14** and **17** and their corresponding lanthanide(III) complexes, and SEM and EDX analyses of Au–Fe_3O_4 NPs. This material is available free of charge via the Internet at http://pubs.acs.org.

AUTHOR INFORMATION

Corresponding Authors

*E-mail: combys7@gmail.com.
*E-mail: gunnlaut@tcd.ie.

Notes

The authors declare no competing financial interest.

ACKNOWLEDGMENTS

The authors thank Cathal McAuley (AML/CRANN) for SEM analyses, Centre for Microscopy and Analysis for TEM measurements and Science Foundation Ireland (Grant SFI PI 2010), and the Irish Research Council (to S.C., E.M.S., O.K. and L.K.T.) for financial support.

REFERENCES

(1) Rosi, N. L.; Mirkin, C. A. *Chem. Rev.* **2005**, *105*, 1547–1562.
(2) Zrazhevskiy, P.; Sena, M.; Gao, X. *Chem. Soc. Rev.* **2010**, *39*, 4326–4354.
(3) Shi, J.; Votruba, A. R.; Farokhzad, O. C.; Langer, R. *Nano Lett.* **2010**, *10*, 3223–3230.
(4) Bamrungsap, S.; Zhao, Z.; Chen, T.; Wang, L.; Li, C.; Fu, T.; Tan, W. *Nanomedicine (London, U.K.)* **2012**, *7*, 1253–1271.
(5) Della Rocca, J.; Liu, D.; Lin, W. *Acc. Chem. Res.* **2011**, *44*, 957–968.
(6) Dreaden, E. C.; El-Sayed, M. A. *Acc. Chem. Res.* **2012**, *45*, 1854–1865.
(7) Adair, J. H.; Parette, M. P.; Altinoglu, E. I.; Kester, M. *ACS Nano* **2010**, *4*, 4967–4970.
(8) Rivera-Gil, P.; Parak, W. J. *ACS Nano* **2008**, *2*, 2200–2205.

(9) Murphy, C. J.; Gole, A. M.; Stone, J. W.; Sisco, P. N.; Alkilany, A. M.; Goldsmith, E. C.; Baxter, S. C. *Acc. Chem. Res.* **2008**, *41*, 1721−1730.
(10) Sperling, R. A.; Riveragil, P.; Zhang, F.; Zanella, M.; Parak, W. J. *Chem. Soc. Rev.* **2008**, *37*, 1896−1908.
(11) Wang, Z.; Ma, L. *Coord. Chem. Rev.* **2009**, *253*, 1607−1618.
(12) Boisselier, E.; Astruc, D. *Chem. Soc. Rev.* **2009**, *38*, 1759−1782.
(13) Cobley, C. M.; Chen, J.; Cho, E. C.; Wang, L. V.; Xia, Y. *Chem. Soc. Rev.* **2011**, *40*, 44−56.
(14) Thakor, A. S.; Jokerst, J.; Zavaleta, C.; Massoud, T. F.; Gambhir, S. S. *Nano Lett.* **2011**, *11*, 4029−4036.
(15) Dykman, L.; Khlebtsov, N. *Chem. Soc. Rev.* **2012**, *41*, 2256−2282.
(16) Llevot, A.; Astruc, D. *Chem. Soc. Rev.* **2012**, *41*, 242−257.
(17) Saha, K.; Agasti, S. S.; Kim, C.; Li, X.; Rotello, V. M. *Chem. Rev.* **2012**, *112*, 2739−2779.
(18) Thomas, K. G.; Kamat, P. V. *Acc. Chem. Res.* **2003**, *36*, 888−898.
(19) Daniel, M. C.; Astruc, D. *Chem. Rev.* **2004**, *104*, 293−346.
(20) Sardar, R.; Funston, A. M.; Mulvaney, P.; Murray, R. W. *Langmuir* **2009**, *25*, 13840−13851.
(21) Bünzli, J. C. *Chem. Rev.* **2010**, *110*, 2729−2755.
(22) McMahon, B.; Mauer, P.; McCoy, C. P.; Lee, T. C.; Gunnlaugsson, T. *J. Am. Chem. Soc.* **2009**, *131*, 17542−17543.
(23) Montgomery, C. P.; Murray, B. S.; New, E. J.; Pal, R.; Parker, D. *Acc. Chem. Res.* **2009**, *42*, 925−937.
(24) Thibon, A.; Pierre, V. C. *Anal. Bioanal. Chem.* **2009**, *394*, 107−120.
(25) Bünzli, J. C.; Eliseeva, S. V. *Chem. Sci.* **2013**, *4*, 1939−1949.
(26) Caravan, P. *Chem. Soc. Rev.* **2006**, *35*, 512−523.
(27) dos Santos, C. M. G.; Harte, A. J.; Quinn, S. J.; Gunnlaugsson, T. *Coord. Chem. Rev.* **2008**, *252*, 2512−2527.
(28) Comby, S.; Bünzli, J.-C. G. Lanthanide Near-Infrared Luminescence in Molecular Probes and Devices. *Handbook on the Physics and Chemistry of Rare Earths*; Gschneidner, K. A., Jr., Bünzli, J.-C. G., Pecharsky, V. K., Eds.; Elsevier Science BV: Amsterdam, The Netherlands, 2007; Vol. *37*, Chapter 235, pp 217−470.
(29) McMahon, B. K.; Gunnlaugsson, T. *J. Am. Chem. Soc.* **2012**, *134*, 10725−10728.
(30) Shinoda, S.; Tsukube, H. *Analyst (Cambridge, U.K.)* **2011**, *136*, 431−435.
(31) Debouttiere, P. J.; Roux, S.; Vocanson, F.; Billotey, C.; Beuf, O.; Favre-Reguillon, A.; Lin, Y.; Pellet-Rostaing, S.; Lamartine, R.; Perriat, P.; Tillement, O. *Adv. Funct. Mater.* **2006**, *16*, 2330−2339.
(32) Alric, C.; Taleb, J.; Le Duc, G.; Mandon, C.; Billotey, C.; Le Meur-Herland, A.; Brochard, T.; Vocanson, F.; Janier, M.; Perriat, P.; Roux, S.; Tillement, O. *J. Am. Chem. Soc.* **2008**, *130*, 5908−5915.
(33) Moriggi, L.; Cannizzo, C.; Dumas, E.; Mayer, C. R.; Ulianov, A.; Helm, L. *J. Am. Chem. Soc.* **2009**, *131*, 10828−10829.
(34) Marradi, M.; Alcantara, D.; de la Fuente, J. M.; Garcia-Martin, M. L.; Cerdan, S.; Penades, S. *Chem. Commun.* **2009**, 3922−3924.
(35) Irure, A.; Marradi, M.; Arnaiz, B.; Genicio, N.; Padro, D.; Penades, S. *Biomater. Sci.* **2013**, *1*, 658−668.
(36) Song, Y.; Xu, X.; MacRenaris, K. W.; Zhang, X. Q.; Mirkin, C. A.; Meade, T. J. *Angew. Chem., Int. Ed.* **2009**, *48*, 9143−9147.
(37) Park, J. A.; Reddy, P. A. N.; Kim, H. K.; Kim, I. S.; Kim, G. C.; Chang, Y.; Kim, T. J. *Bioorg. Med. Chem. Lett.* **2008**, *18*, 6135−6137.
(38) Park, J. A.; Kim, H. K.; Kim, J. H.; Jeong, S. W.; Jung, J. C.; Lee, G. H.; Lee, J.; Chang, Y.; Kim, T. J. *Bioorg. Med. Chem. Lett.* **2010**, *20*, 2287−2291.
(39) Kim, H. K.; Jung, H. Y.; Park, J. A.; Huh, M. I.; Jung, J. C.; Chang, Y.; Kim, T. J. *J. Mater. Chem.* **2010**, *20*, 5411−5417.
(40) Md, N. S.; Kim, H. K.; Park, J. A.; Chang, Y.; Kim, T. J. *Bull. Korean Chem. Soc.* **2010**, *31*, 1177−1181.
(41) Warsi, M. F.; Adams, R. W.; Duckett, S. B.; Chechik, V. *Chem. Commun.* **2010**, *46*, 451−453.
(42) Warsi, M. F.; Chechik, V. *Phys. Chem. Chem. Phys.* **2011**, *13*, 9812−9817.
(43) Ferreira, M. F.; Mousavi, B.; Ferreira, P. M.; Martins, C. I. O.; Helm, L.; Martins, J. A.; Geraldes, C. F. G. C. *Dalton Trans.* **2012**, *41*, 5472−5475.
(44) Lin, M.; Zhao, Y.; Wang, S.; Liu, M.; Duan, Z.; Chen, Y.; Li, F.; Xu, F.; Lu, T. *Biotechnol. Adv.* **2012**, *30*, 1551−1561.
(45) Mader, H. S.; Kele, P.; Saleh, S. M.; Wolfbeis, O. S. *Curr. Opin. Chem. Biol.* **2010**, *14*, 582−596.
(46) Zhou, J.; Liu, Z.; Li, F. *Chem. Soc. Rev.* **2012**, *41*, 1323−1349.
(47) Chen, G.; Ohulchanskyy, T. Y.; Liu, S.; Law, W. C.; Wu, F.; Swihart, M. T.; Ågren, H.; Prasad, P. N. *ACS Nano* **2012**, *6*, 2969−2977.
(48) Wang, G.; Peng, Q.; Li, Y. *Acc. Chem. Res.* **2011**, *44*, 322−332.
(49) Wang, H.; Wang, L. *Inorg. Chem.* **2013**, *52*, 2439−2445.
(50) Liu, Y.; Tu, D.; Zhu, H.; Ma, E.; Chen, X. *Nanoscale* **2013**, *5*, 1369−1384.
(51) Huhtinen, P.; Harma, H.; Lovgren, T. *Recent Res. Dev. Bioconjugate Chem.* **2005**, *2*, 85−108.
(52) Huhtinen, P.; Kivela, M.; Kuronen, O.; Hagren, V.; Takalo, H.; Tenhu, H.; Lovgren, T.; Harma, H. *Anal. Chem.* **2005**, *77*, 2643−2648.
(53) Kokko, L.; Lovgren, T.; Soukka, T. *Anal. Chim. Acta* **2007**, *585*, 17−23.
(54) Hagan, A. K.; Zuchner, T. *Anal. Bioanal. Chem.* **2011**, *400*, 2847−2864.
(55) Pihlasalo, S.; Pellonperä, L.; Martikkala, E.; Hänninen, P.; Härmä, H. *Anal. Chem.* **2010**, *82*, 9282−9288.
(56) Pihlasalo, S.; Kirjavainen, J.; Hänninen, P.; Härmä, H. *Anal. Chem.* **2011**, *83*, 1163−1166.
(57) Pihlasalo, S.; Puumala, P.; Hänninen, P.; Härmä, H. *Anal. Chem.* **2012**, *84*, 4950−4956.
(58) Härmä, H.; Pihlasalo, S.; Cywinski, P. J.; Mikkonen, P.; Hammann, T.; Löhmannsröben, H. G.; Hänninen, P. *Anal. Chem.* **2013**, *85*, 2921−2926.
(59) Mustafina, A. R.; Fedorenko, S. V.; Konovalova, O. D.; Menshikova, A. Y.; Shevchenko, N. N.; Soloveva, S. E.; Konovalov, A. I.; Antipin, I. S. *Langmuir* **2009**, *25*, 3146−3151.
(60) Fedorenko, S. V.; Bochkova, O. D.; Mustafina, A. R.; Burilov, V. A.; Kadirov, M. K.; Holin, C. V.; Nizameev, I. R.; Skripacheva, V. V.; Menshikova, A. Y.; Antipin, I. S.; Konovalov, A. I. *J. Phys. Chem. C* **2010**, *114*, 6350−6355.
(61) Samuel, J.; Tallec, G.; Cherns, P.; Ling, W. L.; Raccurt, O.; Poncelet, O.; Imbert, D.; Mazzanti, M. *Chem. Commun.* **2010**, *46*, 2647−2649.
(62) Gaillard, C.; Adumeau, P.; Canet, J. L.; Gautier, A.; Boyer, D.; Beaudoin, C.; Hesling, C.; Morel, L.; Mahiou, R. *J. Mater. Chem. B* **2013**, *1*, 4306−4312.
(63) Makhinson, B.; Duncan, A. K.; Elam, A. R.; de Bettencourt-Dias, A.; Medley, C. D.; Smith, J. E.; Werner, E. J. *Inorg. Chem.* **2013**, *52*, 6311−6318.
(64) Cousinie, S.; Gressier, M.; Reber, C.; Dexpert-Ghys, J.; Menu, M. J. *Langmuir* **2008**, *24*, 6208−6214.
(65) Divya, V.; Biju, S.; Varma, R. L.; Reddy, M. L. P. *J. Mater. Chem.* **2010**, *20*, 5220−5227.
(66) Duarte, A. P.; Gressier, M.; Menu, M. J.; Dexpert-Ghys, J.; Caiut, J. M.; Ribeiro, S. J. L. *J. Phys. Chem. C* **2012**, *116*, 505−515.
(67) Zhang, D.; Wang, X.; Qiao, Z. A.; Tang, D.; Liu, Y.; Huo, Q. *J. Phys. Chem. C* **2010**, *114*, 12505−12510.
(68) Vivero-Escoto, J. L.; Huxford-Phillips, R. C.; Lin, W. *Chem. Soc. Rev.* **2012**, *41*, 2673−2685.
(69) Chen, Y.; Chi, Y.; Wen, H.; Lu, Z. *Anal. Chem.* **2007**, *79*, 960−965.
(70) Eliseeva, S. V.; Song, B.; Vandevyver, C. D. B.; Chauvin, A. S.; Wacker, J. B.; Bünzli, J.-C. G. *New J. Chem.* **2010**, *34*, 2915−2921.
(71) Duarte, A. P.; Mauline, L.; Gressier, M.; Dexpert-Ghys, J.; Roques, C.; Caiut, J. M.; Deffune, E.; Maia, D. C. G.; Carlos, I. Z.; Ferreira, A. A. P.; Ribeiro, S. J. L.; Menu, M. J. *Langmuir* **2013**, *29*, 5878−5888.
(72) Gao, F.; Luo, F.; Chen, X.; Yao, W.; Yin, J.; Yao, Z.; Wang, L. *Talanta* **2009**, *80*, 202−206.

(73) Qin, P. Z.; Niu, C. G.; Zeng, G. M.; Ruan, M.; Tang, L.; Gong, J. L. *Talanta* **2009**, *80*, 991−995.
(74) Härmä, H.; Keranen, A. M.; Lovgren, T. *Nanotechnology* **2007**, *18*, 075604−1−075604/7.
(75) Xia, X.; Xu, Y.; Zhao, X.; Li, Q. *Clin. Chem.* **2009**, *55*, 179−182.
(76) Wu, J.; Wang, G.; Jin, D.; Yuan, J. G.; Guan, Y. F.; Piper, J. *Chem. Commun.* **2008**, 365−367.
(77) Tian, L.; Dai, Z.; Zhang, L.; Zhang, R.; Ye, Z.; Wu, J.; Jin, D.; Yuan, J. *Nanoscale* **2012**, *4*, 3551−3557.
(78) Philippot, C.; Bourdolle, A.; Maury, O.; Dubois, F.; Boury, B.; Brustlein, S.; Brasselet, S.; Andraud, C.; Ibanez, A. *J. Mater. Chem.* **2011**, *21*, 18613−18622.
(79) Ai, K. L.; Zhang, B. H.; Lu, L. H. *Angew. Chem., Int. Ed.* **2009**, *48*, 304−308.
(80) Sun, Y. Y.; Jiu, H. F.; Zhang, D. G.; Gao, H. G.; Guo, B.; Zhang, Q. J. *Chem. Phys. Lett.* **2005**, *410*, 204−208.
(81) Aslan, K.; Wu, M.; Lakowicz, J. R.; Geddes, C. D. *J. Am. Chem. Soc.* **2007**, *129*, 1524−1525.
(82) Haushalter, J. P.; Faris, G. W. *Appl. Opt.* **2007**, *46*, 1918−1923.
(83) Shukla, R.; Bansal, V.; Chaudhary, M.; Basu, A.; Bhonde, R. R.; Sastry, M. *Langmuir* **2005**, *21*, 10644−10654.
(84) Gu, Y. J.; Cheng, J.; Lin, C. C.; Lam, Y. W.; Cheng, S. H.; Wong, W. T. *Toxicol. Appl. Pharmacol.* **2009**, *237*, 196−204.
(85) Nativo, P.; Prior, I. A.; Brust, M. *ACS Nano* **2008**, *2*, 1639−1644.
(86) Huang, K.; Ma, H.; Liu, J.; Huo, S.; Kumar, A.; Wei, T.; Zhang, X.; Jin, S.; Gan, Y.; Wang, P. C.; He, S.; Zhang, X.; Liang, X. J. *ACS Nano* **2012**, *6*, 4483−4493.
(87) Ojea-Jiménez, I.; Garcia-Fernandez, L.; Lorenzo, J.; Puntes, V. F. *ACS Nano* **2012**, *6*, 7692−7702.
(88) Marchesano, V.; Hernandez, Y.; Salvenmoser, W.; Ambrosone, A.; Tino, A.; Hobmayer, B.; la Fuente, M. d.; Tortiglione, C. *ACS Nano* **2013**, *7*, 2431−2442.
(89) Ipe, B. I.; Yoosaf, K.; Thomas, K. G. *J. Am. Chem. Soc.* **2006**, *128*, 1907−1913.
(90) Lewis, D. J.; Day, T. M.; MacPherson, J. V.; Pikramenou, Z. *Chem. Commun.* **2006**, 1433−1435.
(91) Massue, J.; Quinn, S. J.; Gunnlaugsson, T. *J. Am. Chem. Soc.* **2008**, *130*, 6900−6901.
(92) Lu, Y.; Dasog, M.; Leontowich, A. F. G.; Scott, R. W. J.; Paige, M. F. *J. Phys. Chem. C* **2010**, *114*, 17446−17454.
(93) Anger, P.; Bharadwaj, P.; Novotny, L. *Phys. Rev. Lett.* **2006**, *96*, 113002−1−113002−4.
(94) Jennings, T. L.; Singh, M. P.; Strouse, G. F. *J. Am. Chem. Soc.* **2006**, *128*, 5462−5467.
(95) Dulkeith, E.; Ringler, M.; Klar, T. A.; Feldmann, J.; Munoz Javier, A.; Parak, W. J. *Nano Lett.* **2005**, *5*, 585−589.
(96) Mayilo, S.; Kloster, M. A.; Wunderlich, M.; Lutich, A.; Klar, T. A.; Nichtl, A.; Kürzinger, K.; Stefani, F. D.; Feldmann, J. *Nano Lett.* **2009**, *9*, 4558−4563.
(97) Acuna, G. P.; Bucher, M.; Stein, I. H.; Steinhauer, C.; Kuzyk, A.; Holzmeister, P.; Schreiber, R.; Moroz, A.; Stefani, F. D.; Liedl, T.; Simmel, F. C.; Tinnefeld, P. *ACS Nano* **2012**, *6*, 3189−3195.
(98) Zhang, X.; Marocico, C. A.; Lunz, M.; Gerard, V. A.; Gunko, Y. K.; Lesnyak, V.; Gaponik, N.; Susha, A. S.; Rogach, A. L.; Bradley, A. L. *ACS Nano* **2012**, *6*, 9283−9290.
(99) Bonnet, C. S.; Massue, J.; Quinn, S. J.; Gunnlaugsson, T. *Org. Biomol. Chem.* **2009**, *7*, 3074−3078.
(100) Murray, N. S.; Jarvis, S. P.; Gunnlaugsson, T. *Chem. Commun.* **2009**, 4959−4961.
(101) Molloy, J. K.; Gunnlaugsson, T. Unpublished results, 2010.
(102) Lynch, I.; Dawson, K. A. *Nano Today* **2008**, *3*, 40−47.
(103) De Paoli Lacerda, S. H.; Park, J. J.; Meuse, C.; Pristinski, D.; Becker, M. L.; Karim, A.; Douglas, J. F. *ACS Nano* **2010**, *4*, 365−379.
(104) Hung, A.; Mwenifumbo, S.; Mager, M.; Kuna, J. J.; Stellacci, F.; Yarovsky, I.; Stevens, M. M. *J. Am. Chem. Soc.* **2011**, *133*, 1438−1450.
(105) Monopoli, M. P.; Aberg, C.; Salvati, A.; Dawson, K. A. *Nat. Nanotechnol.* **2012**, *7*, 779−786.
(106) Alkilany, A. M.; Lohse, S. E.; Murphy, C. J. *Acc. Chem. Res.* **2013**, *46*, 650−661.
(107) Comby, S.; Gunnlaugsson, T. *ACS Nano* **2011**, *5*, 7184−7197.
(108) Lewis, D. J.; Bruce, C.; Bohic, S.; Cloetens, P.; Hammond, S. P.; Arbon, D.; Blair-Reid, S.; Pikramenou, Z.; Kysela, B. *Nanomedicine (London, U.K.)* **2010**, *5*, 1547−1557.
(109) Savage, A. C.; Pikramenou, Z. *Chem. Commun.* **2011**, *47*, 6431−6433.
(110) Davies, A.; Lewis, D. J.; Watson, S. P.; Thomas, S. G.; Pikramenou, Z. *Proc. Natl. Acad. Sci. U. S. A.* **2012**, *109*, 1862−1867.
(111) Truman, L. K.; Comby, S.; Gunnlaugsson, T. *Angew. Chem., Int. Ed.* **2012**, *51*, 9624−9627.
(112) Bonnet, C. S.; Gunnlaugsson, T. *New J. Chem.* **2009**, *33*, 1025−1030.
(113) Plush, S. E.; Gunnlaugsson, T. *Dalton Trans.* **2008**, 3801−3804.
(114) Law, G. L.; Pal, R.; Palsson, L. O.; Parker, D.; Wong, K. L. *Chem. Commun.* **2009**, 7321−7323.
(115) Smith, D. G.; McMahon, B. K.; Pal, R.; Parker, D. *Chem. Commun.* **2012**, *48*, 8520−8522.
(116) Weitz, E. A.; Chang, J. Y.; Rosenfield, A. H.; Morrow, E. A.; Pierre, V. C. *Chem. Sci.* **2013**, *4*, 4052−4060.
(117) Truman, L. K.; Gunnlaugsson, T. Unpublished results, 2012.
(118) Jin, Y. *Acc. Chem. Res.* **2013**, DOI: 10.1021/ar400086e.
(119) Liu, Y.; Tu, D.; Zhu, H.; Chen, X. *Chem. Soc. Rev.* **2013**, *42*, 6924−6958.
(120) Feng, W.; Han, C.; Li, F. *Adv. Mater. (Weinheim, Ger.)* **2013**, *25*, 5287−5303.
(121) Tu, D.; Liu, Y.; Zhu, H.; Chen, X. *Chem.—Eur. J.* **2013**, *19*, 5516−5527.
(122) Wang, B.; Hai, J.; Wang, Q.; Li, T.; Yang, Z. *Angew. Chem., Int. Ed.* **2011**, *50*, 3063−3066.
(123) Xi, P.; Cheng, K.; Sun, X.; Zeng, Z.; Sun, S. *Chem. Commun.* **2012**, *48*, 2952−2954.
(124) Liu, Z.; Li, B.; Wang, B.; Yang, Z.; Wang, Q.; Li, T.; Qin, D.; Li, Y.; Wang, M.; Yan, M. *Dalton Trans.* **2012**, *41*, 8723−8728.
(125) Smolensky, E. D.; Zhou, Y.; Pierre, V. C. *Eur. J. Inorg. Chem.* **2012**, 2141−2147.
(126) Smolensky, E. D.; Peterson, K. L.; Weitz, E. A.; Lewandowski, C.; Pierre, V. C. *J. Am. Chem. Soc.* **2013**, *135*, 8966−8972.
(127) Liu, J.; Zhang, W.; Zhang, H.; Yang, Z.; Li, T.; Wang, B.; Huo, X.; Wang, R.; Chen, H. *Chem. Commun.* **2013**, *49*, 4938−4940.
(128) Elmes, R. B. P.; Orange, K. N.; Cloonan, S. M.; Williams, D. C.; Gunnlaugsson, T. *J. Am. Chem. Soc.* **2011**, *133*, 15862−15865.
(129) Lyon, J. L.; Fleming, D. A.; Stone, M. B.; Schiffer, P.; Williams, M. E. *Nano Lett.* **2004**, *4*, 719−723.
(130) Tang, J.; Myers, M.; Bosnick, K. A.; Brus, L. E. *J. Phys. Chem. B* **2003**, *107*, 7501−7506.
(131) Pinna, N.; Grancharov, S.; Beato, P.; Bonville, P.; Antonietti, M.; Niederberger, M. *Chem. Mater.* **2005**, *17*, 3044−3049.
(132) Chourpa, I.; Douziech-Eyrolles, L.; Ngaboni-Okassa, L.; Fouquenet, J.-F.; Cohen-Jonathan, S.; Souce, M.; Marchais, H.; Duboisa, P. *Analyst (Cambridge, U.K.)* **2005**, *130*, 1395−1403.